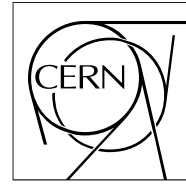


The Compact Muon Solenoid Experiment

CMS Note

Mailing address: CMS CERN, CH-1211 GENEVA 23, Switzerland



06 February 2014 (v3, 18 February 2014)

HE upgrade beyond phase 1. Finger scintillator option.

S.V. Afanasiev, P. de Barbaro, A.Yu. Boyarintsev, I.F. Emeliantchik, I.A. Golutvin, B.V. Grinyov, Yu.V. Ershov, L.G. Levchuk, A.V. Litomin, A.I. Malakhov, P.V. Moisenz, V.F. Popov, N.M. Shumeiko, V.A. Smirnov, P.V. Sorokin, P.N. Zhmurin

Abstract

CMS hadron calorimeters (HB, HE, HO) have been in operation for several years and contributed substantially to the success of the CMS Physics Program. The endcap calorimeter HE suffered more radiation damage than anticipated causing rapid degradation of scintillator segments (tiles) which have a higher radiation flux from secondary particles than HB and HO. A proposal to upgrade of HE calorimeter will provide a solution for survivability at future LHC higher luminosity. A finger-strip plastic scintillator option has many advantages and is a lower cost alternative to keep the excellent HE performance at high luminosity. Measurements and simulations have been performed and this method is a good upgrade strategy.

HE upgrade beyond phase 1. Finger scintillator option.

S.V. Afanasiev^a, P. de Barbaro^e, A.Yu. Boyarintsev^c, I.F. Emeliantchik^d, I.A. Golutvin^a, B.V. Grinyov^c,
Yu.V. Ershov^a, L.G. Levchuk^b, A.V. Litomin^d, A.I. Malakhov^a, P.V. MoisenZ^a, V.F. Popov^b,
N.M. Shumeiko^d, V.A. Smirnov^a, P.V. Sorokin^b, P.N. Zhmurin^c

^a Joint Institute for Nuclear Research, Dubna, Russia

^b National Scientific Center, Kharkov Institute of Physics and Technology, Kharkov, Ukraine

^c Institute for Scintillation Materials National Academy of Sciences of Ukraine, Kharkov, Ukraine

^d National Center for Particle and High Energy Physics, Minsk, Belarus

^e University of Rochester, Rochester, USA

Abstract

CMS hadron calorimeters (HB, HE, HO) have been in operation for several years and contributed substantially to the success of the CMS Physics Program. The endcap calorimeter HE suffered more radiation damage than anticipated causing rapid degradation of scintillator segments (tiles) which have a higher radiation flux from secondary particles than HB and HO. A proposal to upgrade of HE calorimeter will provide a solution for survivability at future LHC higher luminosity. A finger-strip plastic scintillator option has many advantages and is a lower cost alternative to keep the excellent HE performance at high luminosity. Measurements and simulations have been performed and this method is a good upgrade strategy.

1. INTRODUCTION

There are two endcap hadron calorimeters (HE) at each end of CMS and is a part of the hadron calorimeter (HCAL) system of CMS [1, 2]. Both HE's are fine segmented detectors. Each HE is segmented into individual calorimeter cells along three special coordinates: η - pseudorapidity, ϕ - azimuthal angle, and Z along the beam line (see Figure 1). Each endcap has 18 azimuthal (20°) sectors. Every sector has 18 depth layers of scintillators inserted inside brass absorbers. A sector in each layer contains two scintillator trays (megatiles) which are specific in size to that layer.

A single megatile covers ten degrees in the azimuth (see Fig.1). A structure of a single megatile defines a transversal granularity of HE and is divided into 19 cells along η -coordinate and covers η from 1.3 to 3.0. Some HE cells with $\eta = 2.3 - 3.0$ are very close to the beam and are exposed to excessive levels of secondary particles. The high luminosity of the LHC ($\sim 10^{34} \text{ cm}^{-2} \text{ s}^{-1}$) leads to production of plenty of secondary particles. The two endcaps cover a space containing about 34% of the particles produced in pp collisions at the center of CMS [3]. The megatiles (sectional scintillation detectors) of HE irradiated with secondary particles become degraded by the absorbed radiation dose, which is proportional to the total luminosity delivered to CMS, and the damage also depends on the dose rate [4].

Table 1 shows some values of the expected total luminosity and dose rate over time [5].

Table 1.

Years	Instant Luminosity ($\text{cm}^{-2} \text{ sec}^{-1}$)	Total Luminosity (fb^{-1})	Dose Rate (Mrad/hr)
2012	$3.3 \cdot 10^{33}$	23	$1.2 \cdot 10^{-4}$
2015-2018	$1.6 \cdot 10^{34}$	200	$5.8 \cdot 10^{-4}$
2020-2022	$2.5 \cdot 10^{34}$	500	$9.1 \cdot 10^{-4}$
2026-...	$>5.0 \cdot 10^{34}$	3000	$>18.1 \cdot 10^{-4}$

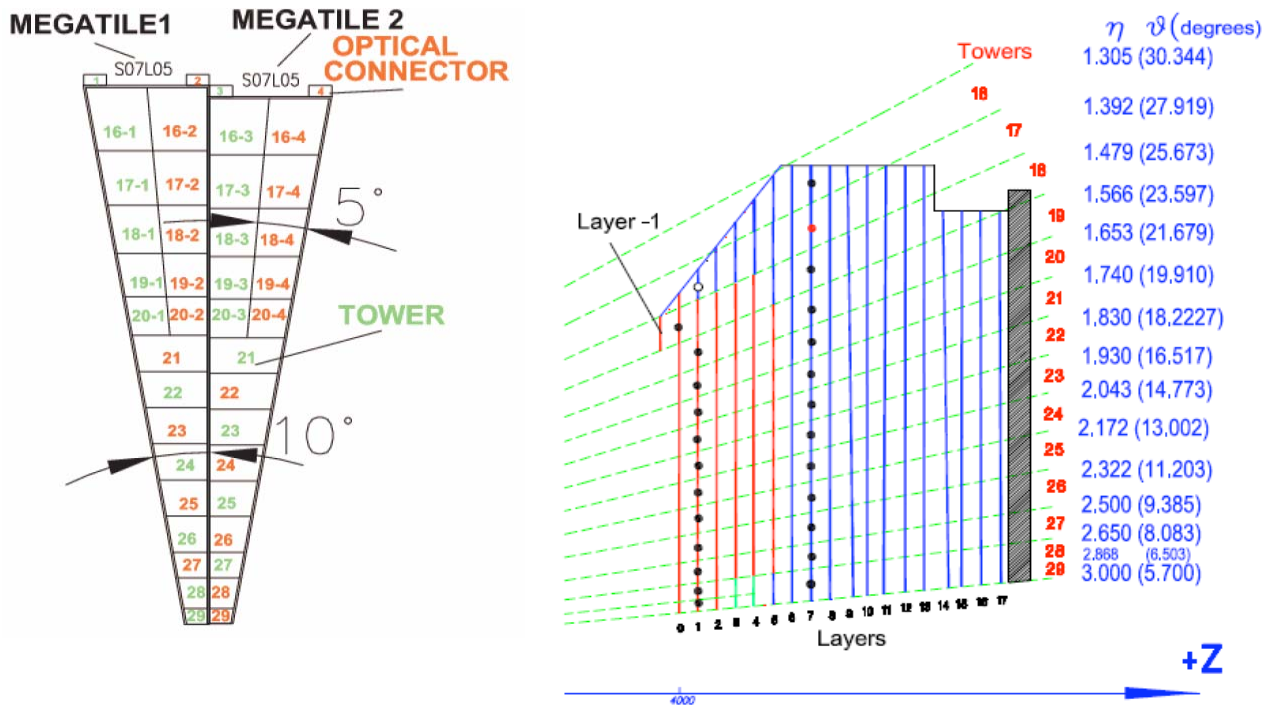


Figure 1. HE segmentation of two adjacent HE scintillator trays and the numbering scheme of layers.

The simulation of HE Radiation dose for 3000 fb^{-1} has been performed by M. Guthoff and A. Dabrowski [6]. The results of simulation are shown in Figure 2.

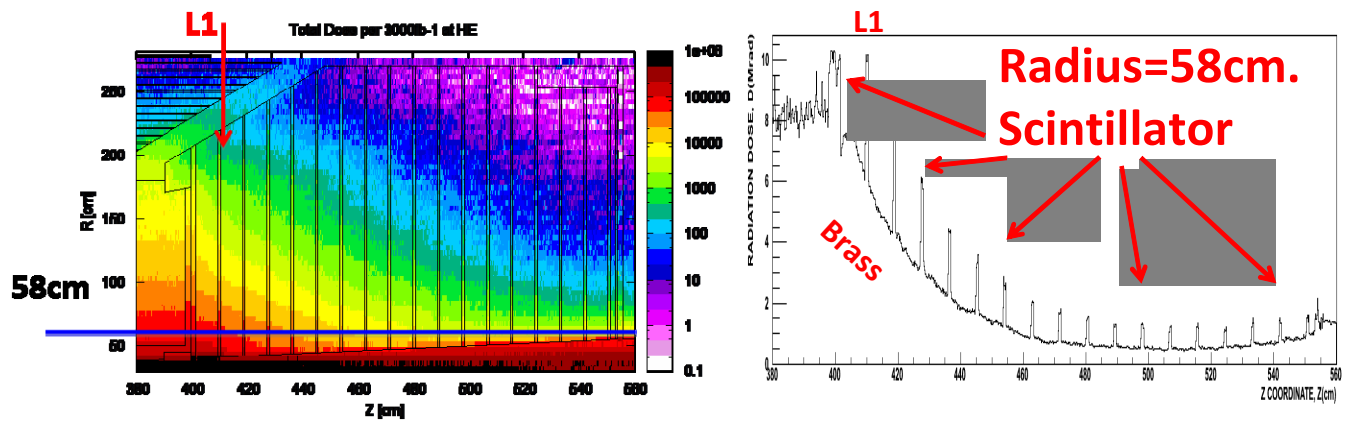


Figure 2. Total absorbed dose in HE vs coordinates Z and R for 3000 fb^{-1} .

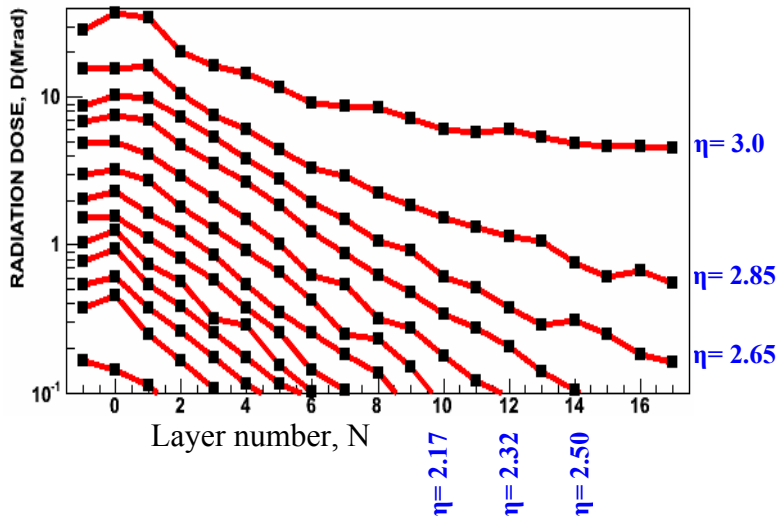


Figure 3. Distribution of absorbed dose for individual cells of HE.

The distribution of the absorbed dose for cells (tiles) of HE megatile according to its η and layer number is shown in Figure 3. The simulation has shown that the most irradiated cells of HE are located in layer 1. Figure 4 shows the calculated values of the absorbed dose and dose rates for tiles 26 – 29 at LHC luminosity of 3000 fb^{-1} . The initial estimates of the light yield have predicted that HE scintillator/WLS fibers will have only moderate radiation damage up to 500 fb^{-1} (10 year of LHC operation at design luminosity) [7, 8]. In order to provide HE operation at high luminosity of LHC (3000 fb^{-1}), a limited number of tiles in high-eta front layers of HE would have to be replaced. Analysis of 2012 CMS data has shown that radiation damage in HE is much faster and deeper than initially expected (see Figure 5).

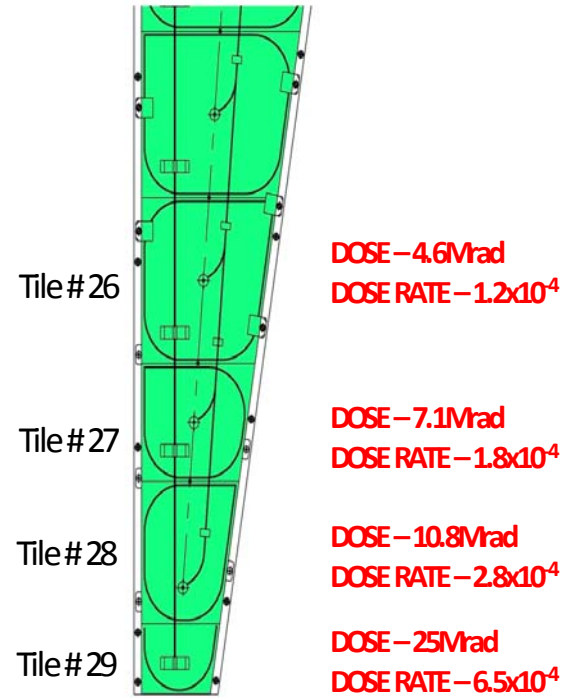
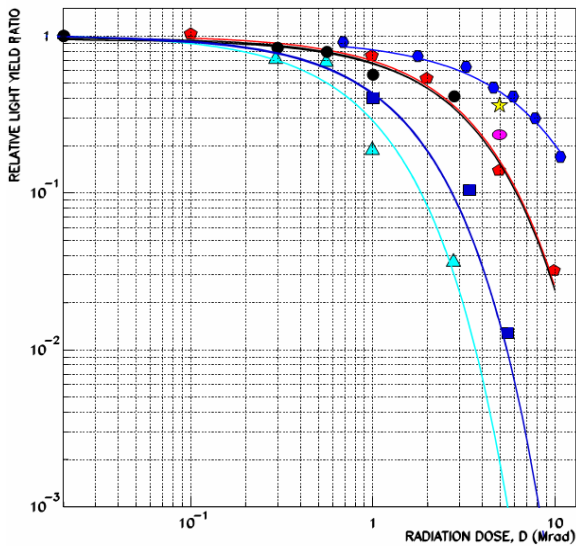


Figure 4. Schematic view of tiles 26 -29 in HE megatile and the calculated values of the absorbed dose and dose rates (Mrad/hr) for each selected tile each selected tile.



- SCSN-81 & BCF-91, 10x10cm, CMS HCAL TDR [7]
- ★ SCSN-81 & Y11, ~6x8cm, Co60 irradiation, Protvino, 2011 year [11]
- SCSN-81 & Y11, 10x10cm, e irradiation, (15mm from shifter), Dubna [10]
- ◆ SCSN-81 & Y11, 12x8cm, Co60 irradiation, 1 week after irradiation [8]
- ▲ SCSN-81 & Y11(.85mm), tile 27, e irradiation, immediately after irradiation
- SCSN-81 & Y11(.85mm), tile 27, e irradiation, 5-7 days after irradiation
- SCSN-81 & 8 shifters Y11(1mm), tile N27, e irradiation, immediately after irradiation

Figure 5. Relative light yield ratio vs. the radiation dose (fit by exponential form).

2. The stripped tile -- “fingers” advantages in high radiation environment.

The plastic scintillator absorbs radioactive doses during its operation as a detector in HEP spectrometers. The life-time of plastic scintillators depends on the quantity of the absorbed dose and dose rate. The main idea is to provide a solution to the plastic scintillators at high radiation to survive as long as possible. A design of the plastic detector (the shape and position of WLS fibers) should provide the best light collection. The WLS fiber collects the light produced by the charged particles which pass through the scintillator. It is spliced to a clear fiber; its other end is connected to the Photo Detector. The irradiation affects both the scintillator and WLS fiber. Degradation of the scintillators and WLS fibers means decreasing in the number of photons arriving at the Photo Detector. The factors of light losses together with the dose increase are caused by the following reasons:

1. Transmittance loss in the scintillator (becomes yellow).
2. Transmittance loss in the WLS fiber.
3. Degradation of scintillating emission.
4. Reduction of conversion efficiency of WLS fiber.

The improvement in light collection may be provided by reducing the size of the scintillator segments [9, 10]. The tiles (24 – 29), which are close to the beam line and accumulate more doses, are proposed to compose to change from one to 4 or 8 equal segments (see Figure 6). Each segment will have its own WLS fiber. The width of the segment is defined as one-fourth or one-eighth of the azimuthal size of the tile. WLS fiber in the segment is laid straightly along the long side and is mounted in its center. The impact of scintillation darkening is reduced because an average path length of light from the emission point to the WLS fibers is shorter. The length of WLS fibers also becomes shorter, and, hence, the loss of light caused by its darkening reduces. The light from all segments of a tile is combined to a single new photo detector made of silicon SiPM.

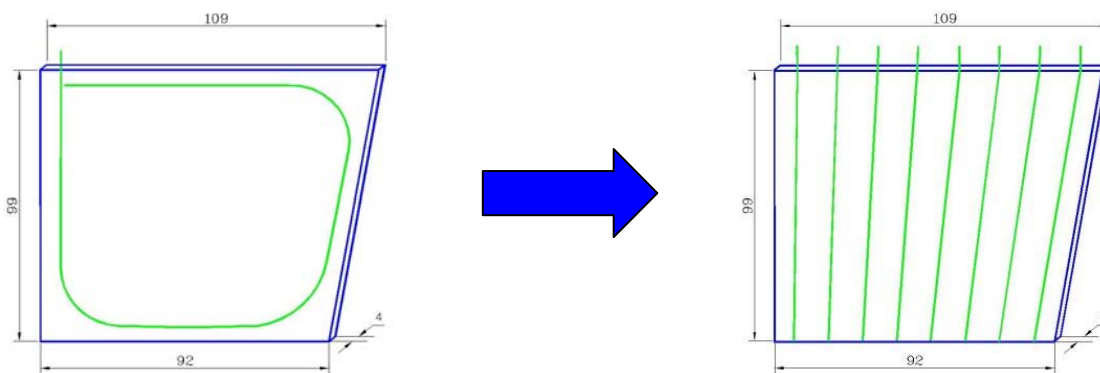
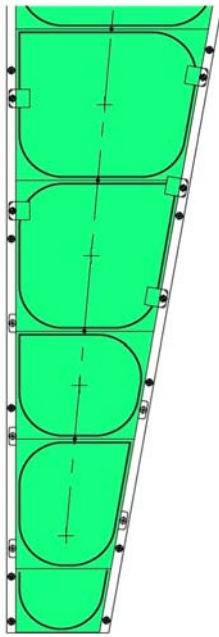


Figure 6. Main concept of tile transformation from a scintillator tile with the basic structure to the stripped tile – array of fingers.

It is proposed to replace 4 tiles (26, 27, 28, 29) in each megatile of the first 5 layers (0 – 4) with the finger design. Figure 7 demonstrates these changes. The number of clear fibers between the stripped tiles and the optical connectors located on the edge of the megatile is increased. Table 2 shows the distribution of fibers in two optical connectors of the current megatile. The increased number of fibers needs the installation of two additional 12-pin optical connectors for layers 1 – 4 and four for layer 0 on the edge of each modified megatile. It also requires modification of the fiber layout in two existing connectors (see Table 3).

The additional optical lines between the megatile and RM should be laid (see Table 4) and six additional 12-pins optical connectors should be located on each RM. Figure 8 shows a view of optical connectors on the current HE RM.

Existing tiles granulation



Tile # 25

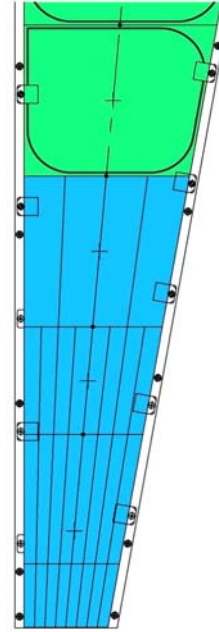
Tile # 26

Tile # 27

Tile # 28

Tile # 29

New fingers granulation option



4 fingers

8 fingers

8 fingers

8 fingers

Figure 7. Finger scintillator concept.

Table 2.

Connector 1 (12-pin)

L04	29	27	25	23	21	20	19	18	17	16		
L03	29	27	25	23	21	20	19	18	17	16		
L02	29	27	25	23	21	20	19	18	17			
L01	29	27	25	23	21	20	19	18	17			
L00	29	27	25	23	21	20	19	18	17	CL		
L0	29	27	25	23	21	20	19	18	17			
L-1						18						

Connector 2 (12-pin)

			16	17	18	19	20	22	24	26	28	
			16	17	18	19	20	22	24	26	28	
				17	18	19	20	22	24	26	28	
				17	18	19	20	22	24	26	28	
				17	18	19	20	22	24	26	28	
				17	18	19	20	22	24	26	28	
				18								

Table 3.

Connector 1 (12-pin)

L04	29/1	27/1	25	23	21	20	19	18	17	16		
L03	29/1	27/1	25	23	21	20	19	18	17	16		
L02	29/1	27/1	25	23	21	20	19	18	17			
L01	29/1	27/1	25	23	21	20	19	18	17			
L00	29/1	27/1	25	23	21	20	19	18	17	CL		
L0	29/1	27/1	25	23	21	20	19	18	17			
L-1						18						

Connector 1d (12-pin)

	29/2	29/3	29/4	28/1	28/2	28/3	28/4	27/2	27/3	27/4	26/1	26/2
	29/2	29/3	29/4	28/1	28/2	28/3	28/4	27/2	27/3	27/4	26/1	26/2
	29/2	29/3	29/4	28/1	28/2	28/3	28/4	27/2	27/3	27/4	26/1	26/2
	29/2	29/3	29/4	28/1	28/2	28/3	28/4	27/2	27/3	27/4	26/1	26/2
	29/2	29/3	29/4	28/1	28/2	28/3	28/4	27/2	27/3	27/4	26/1	26/2
	29/2	29/3	29/4	28/1	28/2	28/3	28/4	27/2	27/3	27/4	26/1	26/2

Connector 2d (12-pin)

L04	26/3	27/5	27/6	27/7	27/8	28/5	28/6	28/7	29/5	29/6	29/7	29/8
L03	26/3	27/5	27/6	27/7	27/8	28/5	28/6	28/7	29/5	29/6	29/7	29/8
L02	26/3	27/5	27/6	27/7	27/8	28/5	28/6	28/7	29/5	29/6	29/7	29/8
L01	26/3	27/5	27/6	27/7	27/8	28/5	28/6	28/7	29/5	29/6	29/7	29/8
L00	26/3	27/5	27/6	27/7	27/8	28/5	28/6	28/7	29/5	29/6	29/7	29/8
L0	26/3	27/5	27/6	27/7	27/8	28/5	28/6	28/7	29/5	29/6	29/7	29/8
L-1						18						

Connector 2 (12-pin)

			16	17	18	19	20	22	24	26	28	
			16	17	18	19	20	22	24	26	28	
				17	18	19	20	22	24	26	28	
				17	18	19	20	22	24	26	28	
				17	18	19	20	22	24	26	28	
				17	18	19	20	22	24	26	28	
				18								

Table 4.

Layers	Optical cable from connector 1, # of fibers	Optical cable from connector 2, # of fibers	Optical cable from connector 1d, # of fibers	Optical cable from connector 2d, # of fibers
L0	9	8	12	12
L00	9	8	12	12
L1	9	8	12	12
L2	9	8	12	12
L3	10	9	12	12
L4	10	9	12	12



Figure 8. A view of the unmodified front panel on HE RM.

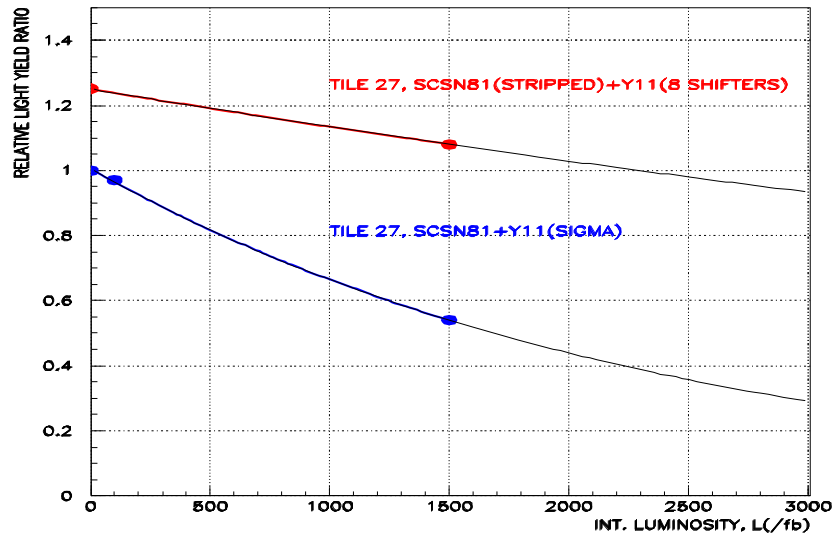


Figure 9. Relative light yield vs int. luminosity for neutrons

The irradiation by neutrons at the reactor (JINR, Dubna) and the following measurements of the original scintillator tile with the basic structure and stripped tile were performed. The original tile is identical to tile 27 in which WLS fiber is located as shown in Figure 6 left. Figure 9 demonstrates an advantage of finger options i.e. the gain in the light yield for equal irradiation conditions.

2. Main problems in plastic scintillator damage.

The previous and current studies of plastic scintillator damage caused by radiation have shown that this damage is a complex function of Dose and Dose Rate. The direct measurement of this phenomenon is not possible. It takes too long – years. There are still three issues to be considered:

1. Radiation damage of “fingers” at 2500-3000 fb⁻¹ (survivability by the end of LHC).
2. Radiation damage of existing sigma tiles at 700 fb⁻¹(survivability to the LS3).
3. Understanding of SCSN81/Y11 radiation damage at 30 fb⁻¹(2011 and 2012 runs).

3. Program of scintillator/WLS radiation damage study.

There are several irradiation facilities at the Joint Institute for Nuclear Research (JINR, Dubna) and its member states. JINR has two large-scale neutron sources: the IBR-2 pulsed fast neutron reactor (with the highest neutron flux in pulse among the world’s neutron sources) and the Intense REsonance Neutron source (IREN).

The IBR-2 reactor [12] with its unique technical approach produces one of the most intensive pulse neutron fluxes at the moderator surface among the world's reactors:

- Primary flux: $n(85\%)+\gamma(15\%) 10^9-10^{11} \text{ cm}^{-2}\text{s}^{-1}$ ($\langle E_n \rangle \sim 1\text{MeV}$)
- Dose rate: $500 \text{ kRad h}^{-1} (\langle E_\gamma \rangle \sim 1.5-2 \text{ MeV})$
- Fluence: $\sim 3 \cdot 10^{15} \text{ n/cm}^2$ in per run

Figure 10 shows the neutron instrumentation at the IBR-2 reactor.

The research complex IREN [13] is one of the JINR basic facilities. IREN is still in the construction phase, but the first stage of the complex is available for experimental research. IREN is based on the electron linear accelerator and contains a non-multiplying neutron producing target. The achieved parameters are as follows:

- Total neutron intensity: $\sim 10^{11} \text{ s}^{-1}$ ($\langle E_n \rangle \sim 1\text{MeV}$)
- Total gamma intensity: $\sim 3 \cdot 10^{13} \text{ s}^{-1}$
- Dose rate: $0 \div 340 \text{ kRad h}^{-1} (\langle E_\gamma \rangle \sim 1.5-2 \text{ MeV})$

The material of the neutron producing target is a tungsten based alloy. It is formed as a cylinder 40 mm in diameter and 100 mm height spaced within the aluminum can, 160 mm in diameter and 200 mm height (see Figure 11).

Kharkov Institute of Physics and Technology (KIPT) is one of oldest and largest energy centers of physical science in Ukraine. Figure 12 shows the experimental area of KIPT LINAC (10 MeV electron linac), which has the following main parameters [14]:

- Beam: 9.1÷9.4 MeV
- Beam current : $820 \mu\text{A}$
- Dose rate: $0.018 \div 800 \text{ Mrad/h}$

The 4 MeV electron linac of the National Center for Particle and High Energy Physics in Minsk, Belarus, has the following parameters:

- Beam energy: 4 MeV
- Beam intensity : $8 \cdot 10^{11} \text{ cm}^{-2}\text{s}^{-1}$
- Dose rate: up to 100 Mrad/h

The material used for irradiation is as follows: scintillators SCSN-81, UPS-923A, Bicron BC-408; WLS fibers Y11 ($d=0.85 \text{ mm}$, $d=0.98 \text{ mm}$) and clear fiber BCF-98.

Several sets of test samples were prepared:

- sigma tiles (see Figure 6) with dimensions close to tile #27 in the layer #1 with WLS fiber Y11 $d=0.85 \text{ mm}$;
- finger type scintillators (length $60 \div 148 \text{ mm}$, width $12 \div 20 \text{ mm}$, thickness 4 mm);
- “squares” samples ($32 \times 32 \text{ mm}^2$) of SCSN-81 and UPS-923A and $25 \times 25 \text{ mm}^2$ of SCSN-81. The thickness is about 4 mm;
- WLS fibers spliced with clear fibers.

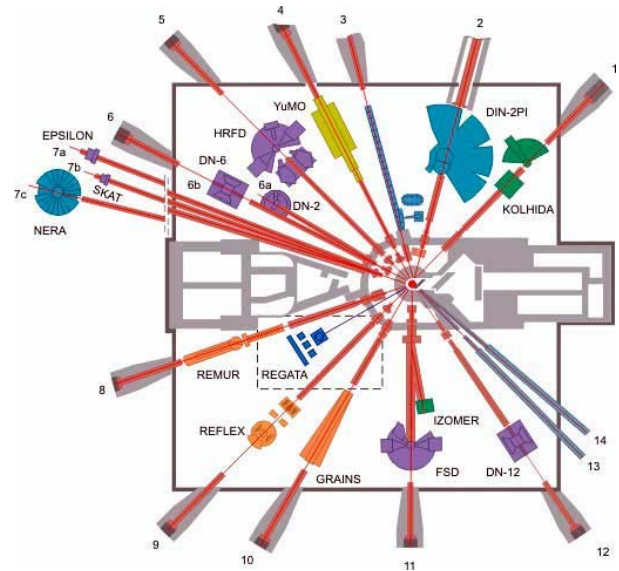


Figure 10. Layout of IBR.

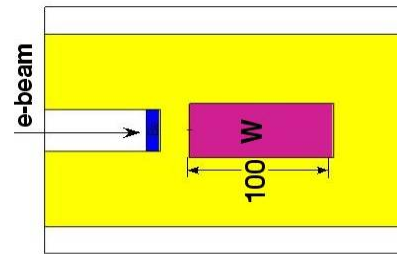


Figure 11. A schematic view of the neutron producing target.

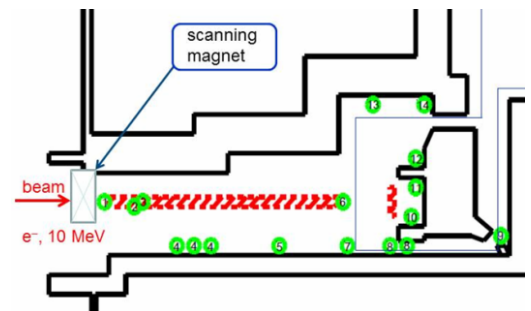


Figure 12. Experimental area of KIPT LINAC.

Several assemblies of the megatiles prototypes will be prepared. Each of them is composed of four tiles (#26 ÷ #29), the same as for layer 1, and has the finger structure. The irradiation of samples proposed to perform in the atmosphere of both Nitrogen and Air.

The research program plans to irradiate samples with a different dose rate in the range from 0.00025 up to 0.338 Mrad/hr. Each radiation exposure will take 90 days. The following procedures should be performed:

- Irradiation of “sigma” tiles up to dose 0.3 Mrad that will allow one to understand the radiation damage of SCSN-81/Y11 assembly for the 30 fb-1 integrated luminosity.
- Irradiation of “sigma” tiles up to dose 5.0 Mrad that will allow one to predict the properties of existing tiles up to 500-700 fb⁻¹ of the integrated luminosity.
- Irradiation of the “finger” type tiles up to dose 25 Mrad that will allow one to predict the radiation damage of new tiles up to 2500-3000 fb-1 of the integrated luminosity.
- Irradiation of “squares” samples up to the dose of 25 Mrad that will allow one to understand the properties of the scintillator as function of the dose rate and absorbed dose.
- Irradiation of “squares” samples in the nitrogen atmosphere that will allow one to determine the effect of gas environment on recovery processes in the scintillator.
- Irradiation of the “prototype” at the minimal dose rate up to dose 25 Mrad. It is a complex test of the radiation resistance of the modified tiles.

The goal of the program is to extrapolate the results of measurement for real conditions of CMS operation in 2012 – 2030.

4. Experimental results of studying the scintillator/WLS radiation damage.

This program is in progress. Below we present some of the experimental results which have been already obtained. Several samples of the SCSN-81 (Kuraray) and UPS-923A (Kharkov) scintillators were prepared and irradiated at the KIPT 10 MeV electron linac (electrons + photons) to the doses of 1.7 and 4.3 Mrad at the rates of 0.02, 0.12 and 0.2 Mrad/hr. The exact beam energy (from 9.1 to 9.4 MeV) was under control, and the average beam current was 820 mA. Reasonable irradiation uniformity over the target surface was also provided. The irradiation dose was measured by the Harwell Red 4034 dosimeters. Several types of scintillator samples were studied. One of them (see Figure 13a) was a 4 mm thick square (32×32 mm²) plate. Another one was a 4 mm thick disc with a diameter of 30 mm (see Figure 13b). For the light yield measurements before and after irradiation the samples were attached directly to the PMT (see Figure 14).

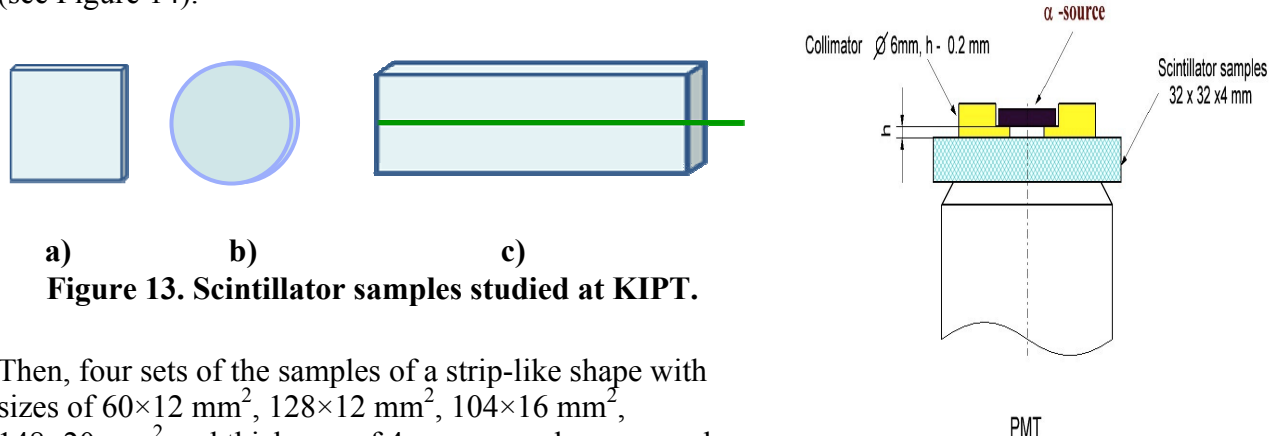


Figure 13. Scintillator samples studied at KIPT.

Figure 14. Light yield measurement layout.

Then, four sets of the samples of a strip-like shape with sizes of 60×12 mm², 128×12 mm², 104×16 mm², 148×20 mm² and thickness of 4 mm were also prepared and studied. In this case the light was transferred to the PMT through the WLS fiber (Kuraray Y11) inserted into the groove in the middle of the strip (see Figure 13c).

Figure 15 shows the dependence of light yield from the samples on the dose rate. Light yield degradation under irradiation turns out to be substantially greater at lower rates. The KIPT data are in a good agreement with the earlier experimental results [4]. Since the estimated dose rate at the HE for the HL-LHC conditions does not exceed ~ 1 krad/hr, the dose rate effect being discussed here needs to be taken into account in the HCAL Upgrade Project.

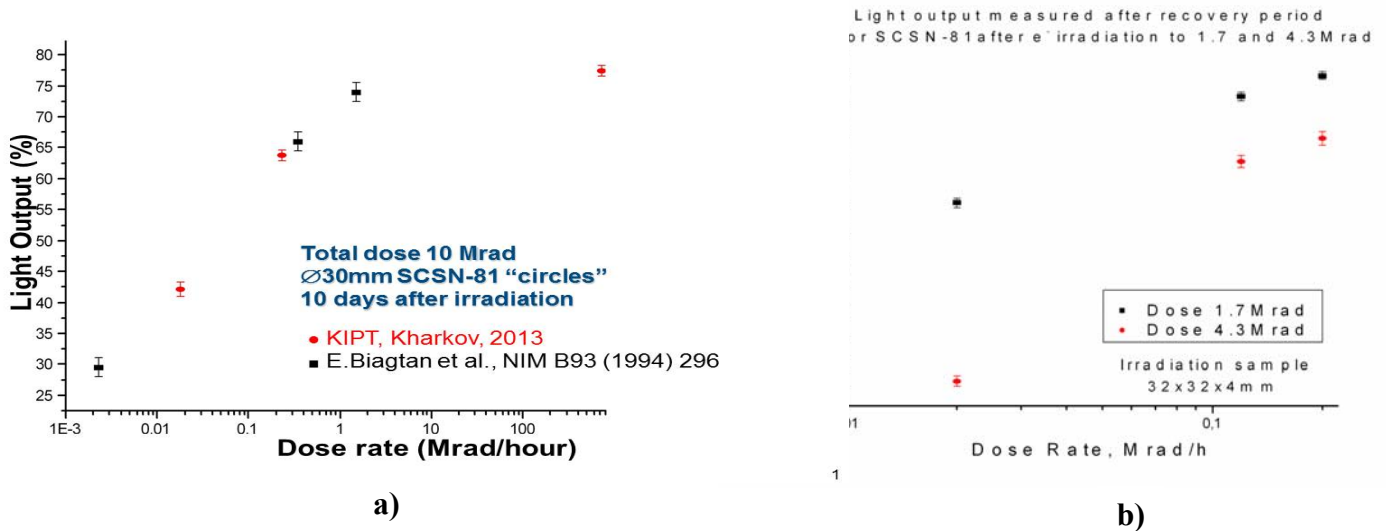


Figure 15. Light yield degradation under irradiation vs. dose rate for SCSN-81 samples irradiated to 10 Mrad (a) and to 1.7 and 4.3 Mrad (b).

Preliminary predictions of the relative light yield for 30 fb^{-1} and 500 fb^{-1} (SCSN81, tile#29, layer#1) are shown in Figure 16. The above mentioned KIPT experimental results (marked as ● and ■) are used as the basis to calculate some predictions (marked as ●, ■, and ■).

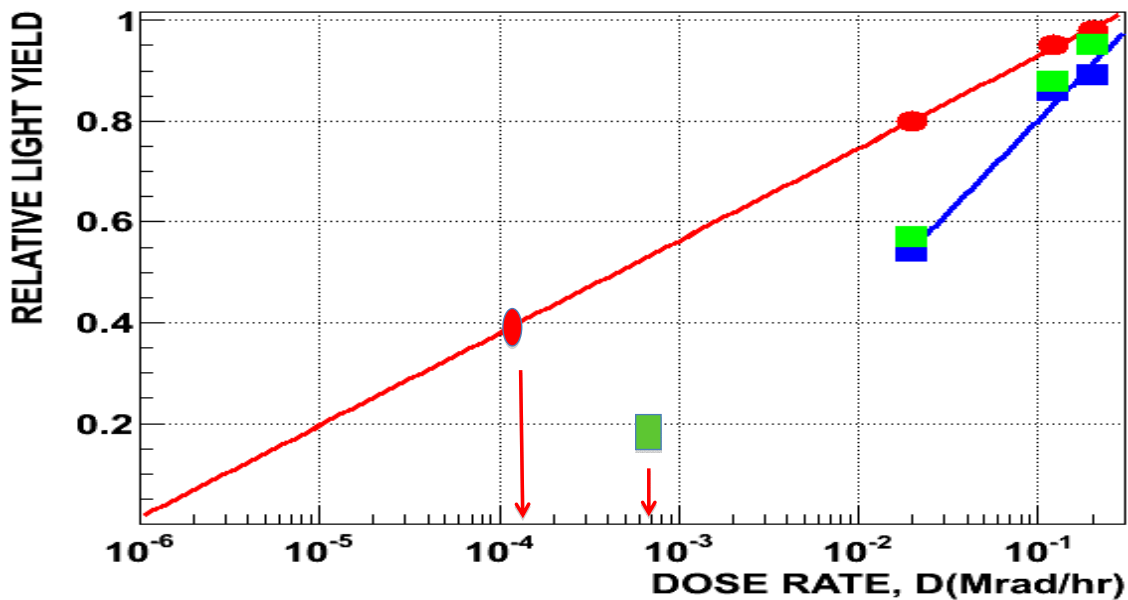


Figure 16. KIPT experimental results and some preliminary predictions of the relative light yield for 30 fb^{-1} and 500 fb^{-1} .

The results of measurements ● and ■ are received after irradiation of square scintillator samples ($32 \times 32 \text{ mm}^2$) with the absorption doses 1.7 Mrad and 4.3 Mrad accordingly for three different values of the dose rate. Calculations of the relative light yield for the absorption dose of 4.3 Mrad on the basis of the 1.7 Mrad (■) data have been performed. They have shown a very good agreement with the real measured data for 4.3 Mrad and have given a confidence to predict the relative light yield for different levels of the absorption dose and dose rate. WLS fiber degradation was not taken into account in this

extrapolation. The predicted data marked as ● have been calculated for the absorption dose of 1.7 Mrad and the dose rate of $1.25 \times 10^{-4} \text{ Mrad/hr}$, it was done in 2012. The next prediction was done for the same dose rate, but for the integral luminosity of 30 fb^{-1} . In this case the calculated value of the relative light yield for tile 29 is equal to 0.71. It means that the absorbed dose in tile 29 is considerably less than 1.7 Mrad. The predicted data marked as ■ have been calculated for the absorbed dose of 4.3 Mrad and for the dose rate of $6.4 \times 10^{-4} \text{ Mrad/hr}$ that will be expected just before LS3. The next prediction was done for the same dose rate, but for the integral luminosity of 500 fb^{-1} . In this case the calculated value of the relative light yield for tile 29 is equal to 0.016.

These predictions are in a good agreement with the CMS experimental results, but it is very important to provide additional experimental points near 10^{-3} Mrad/hr .

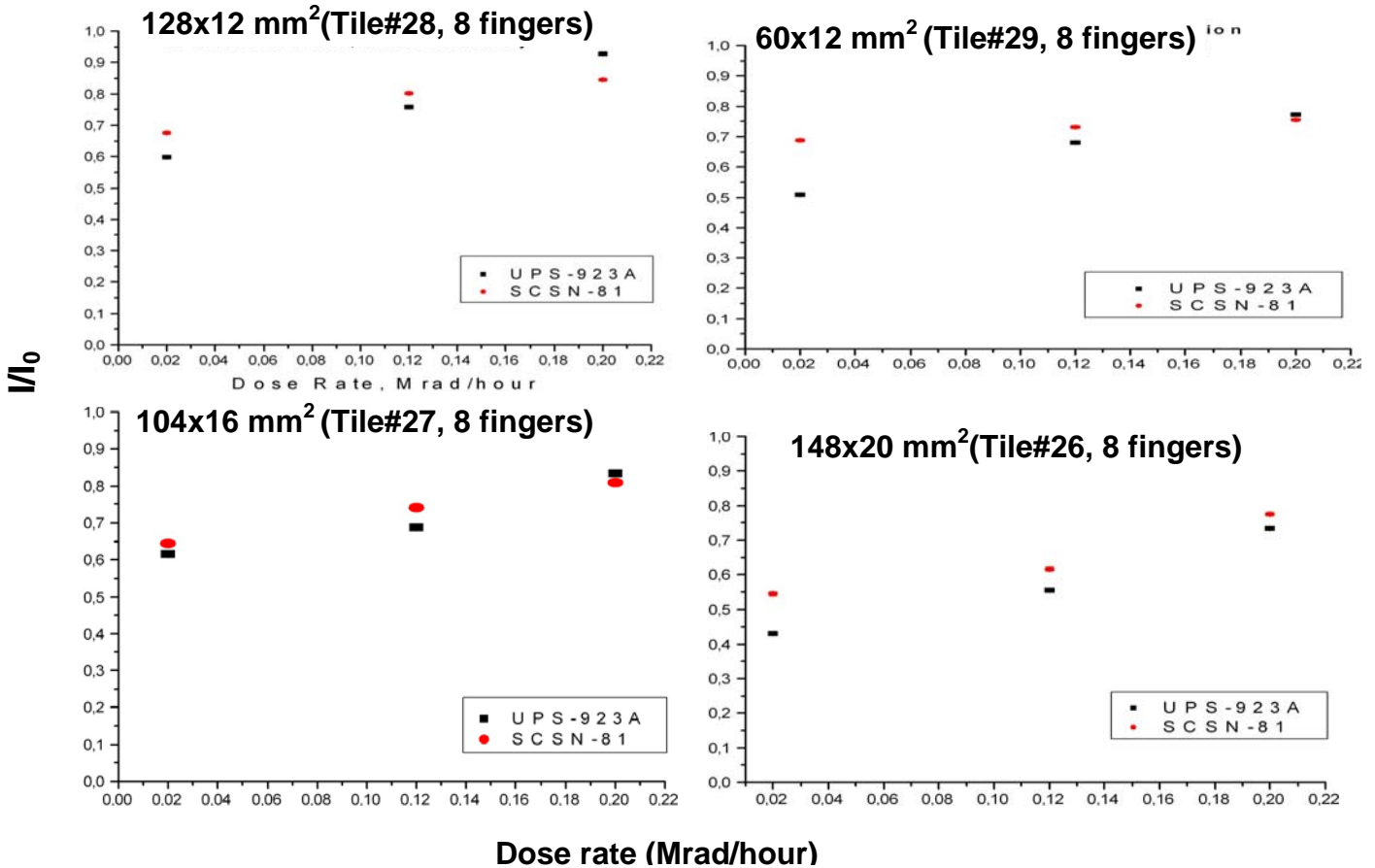


Figure 17. Light yield degradation under irradiation vs. dose rate for SCSN-81 and UPS-923A “finger strips” irradiated to 1.7 Mrad.

For the KIPT studies of the finger-strip samples, the WLS was used in the readout but not exposed. The SCSN-81 and UPS-923A samples were exposed to the dose of 1.7 Mrad, and the light yield was being measured for 10 days after the irradiation. The strip sizes corresponded to the ones for tiles 26, 27, 28 and 29 (see Figure 7). The results of the measurements shown in Figure 17 indicate a substantial dependence

of the dose rate effect on the strip size. Further studies of this dependence are needed to optimize the finger strip geometry.

Measurements were also performed on WLS fibers, type Y11, at the National Center for Particle and High Energy Physics, Minsk, Belarus. The measurements have been performed using the electron beam at the energy of 4 MeV. Figure 18a shows the results of light yield measurements from the irradiated WLS fiber for several values of the absorbed dose and with the constant dose rate value of 90 Mrad/hr. The degradation effect increases with the accumulated dose. Figure 18b shows the behavior of WLS fibers during the annealing period after irradiation. These measurements are in a fair agreement with the earlier KIPT results. Y11 WLS fiber does not have much of any dose rate dependence.

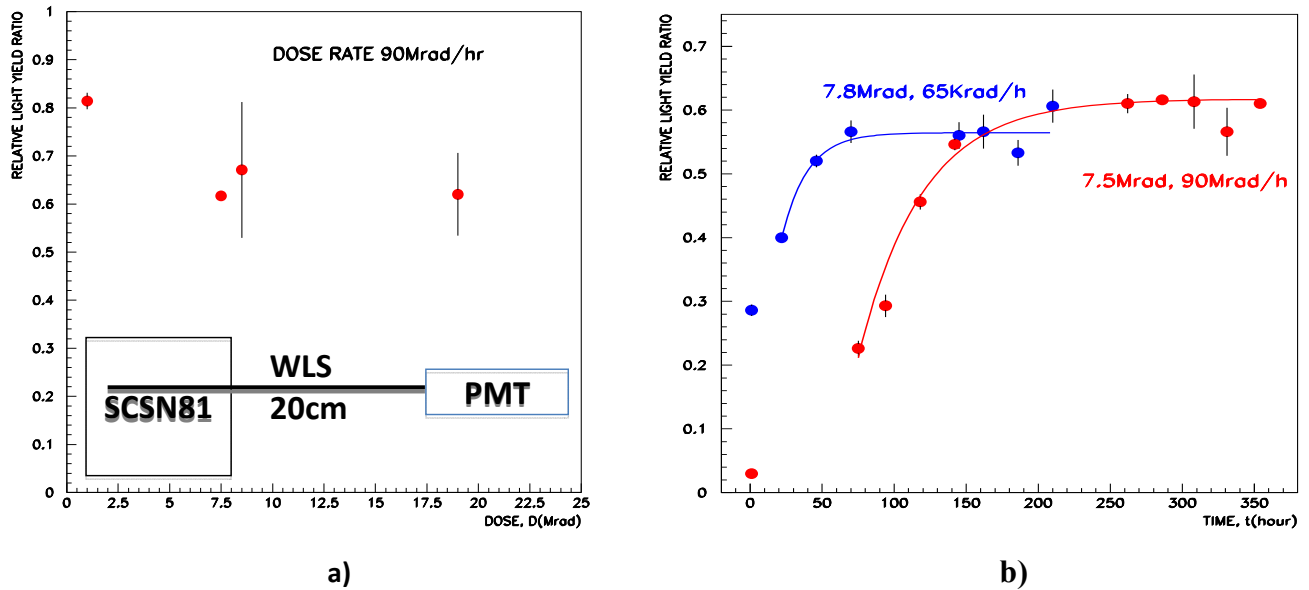


Figure 18. Results of light yield measurements from the irradiated WLS fiber (Minsk).

A considerable increase of the light yield may be achieved by radiation of the hard 3 HF scintillator and WLS fiber O2 [15].

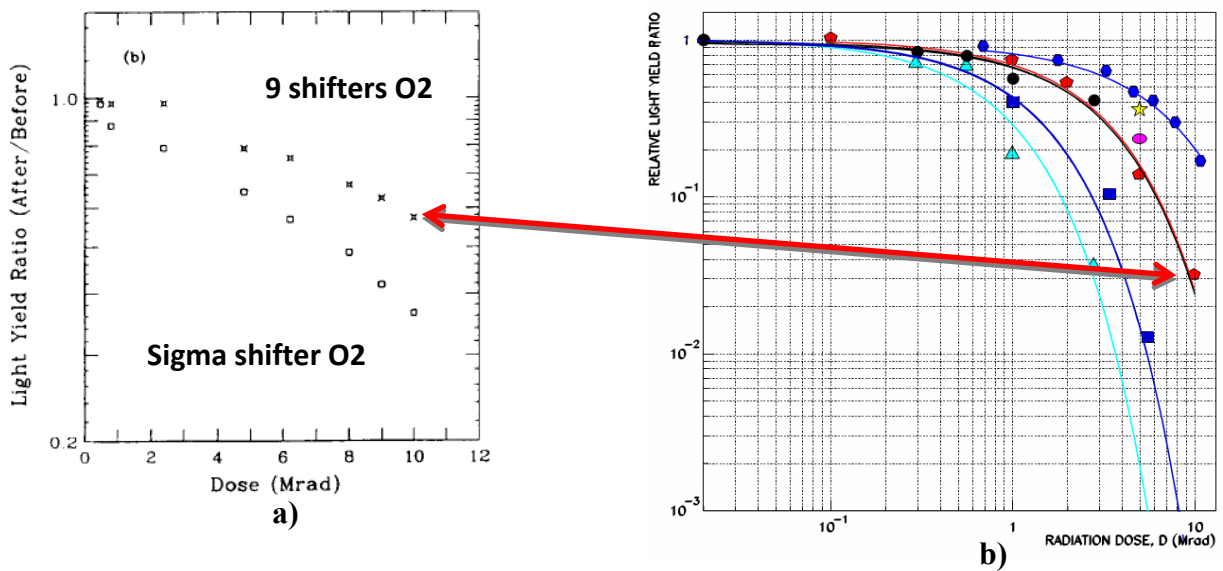


Figure 19. Comparison of light yield results for 3 HF tile composed of 9 strips with current CMS collaboration results.

The 3 HF scintillator emits in the green light. O2 WLS fiber shifts from the green to the orange light. A combination of 3 HF with O2 WLS and multi-fiber light collection from the tile can provide an assembly with the increased radiation hardness. Figure 19a shows the better results of the light yield for 3 HF scintillating tile composed of 9 strips in comparison with the usual one [15]. Figure 19b is the same as Figure 5. The BEPC electron beam (1.1 – 1.3 GeV) was used to irradiate the modules. Each module consists of 21 Pb absorber plates (5 mm thick, 12.7 cm X 12.7 cm in area) interspersed with 20 polystyrene-based scintillator tiles (2.6 mm thick, 11 cm X 11 cm in area). The WLS fibers, 1 mm in diameter, are embedded in the scintillator tiles without glue. These fibers collect light from the scintillator tiles and transfer it to photomultiplier tubes (PMT) via a high transmittance clear fiber spliced to the WLS fiber. Figure 19b shows the current CMS collaboration results.

Development and production of a new scintillator can be done at the Institute of Scintillation Material (ISMA, Kharkov).

Irradiation of HE scintillator tiles also takes place in the absence of the beam due to the induced radioactivity of the absorber. Figure 20 shows the results of the simulation of the dose rate ($\mu\text{ Sv/h}$) caused by the induced radioactivity of the HE absorber after 4 weeks of cooling in LS1, LS2 and LS3 long shut-downs. The simulation has been done by C. Urscheler and H. Vincke.

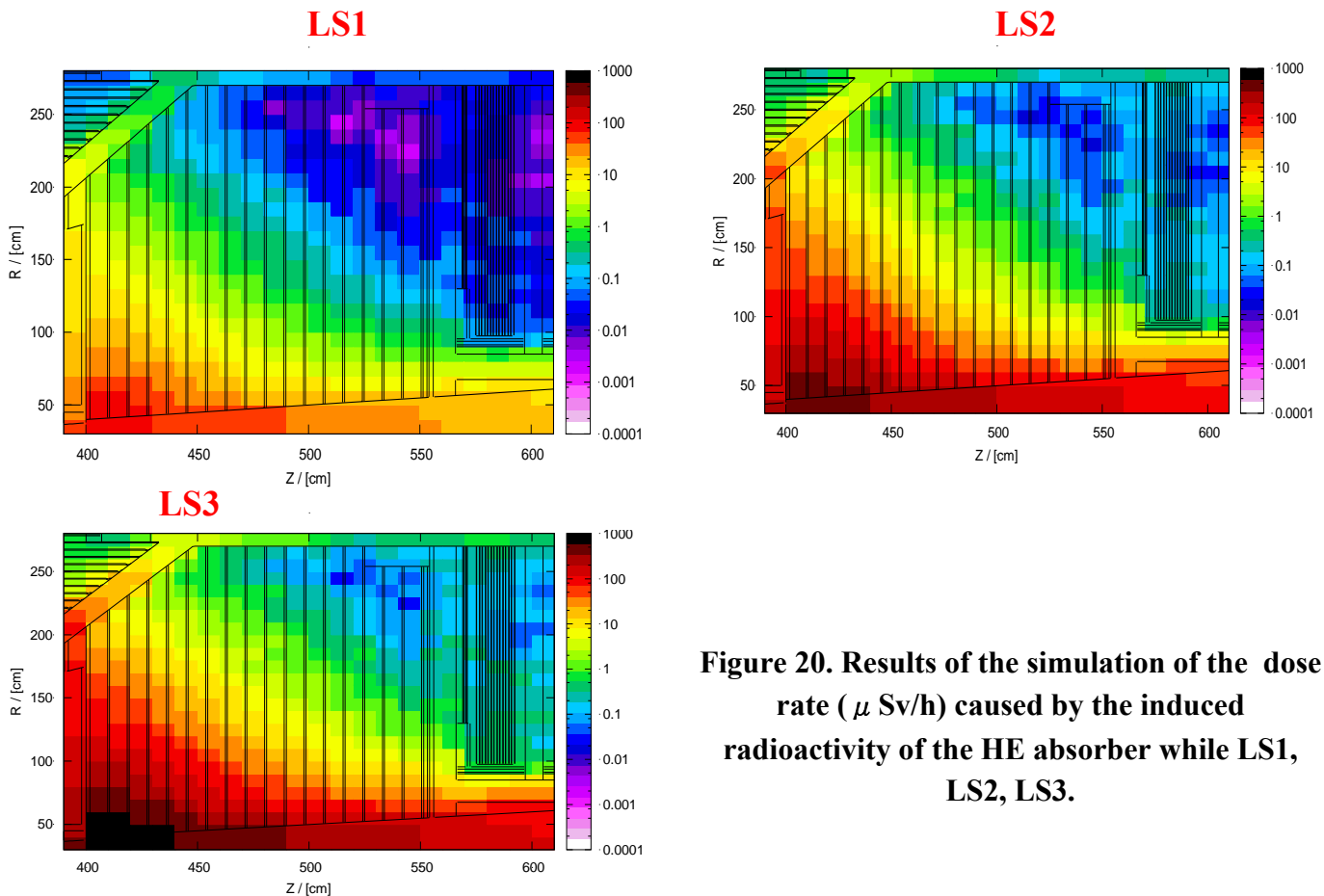
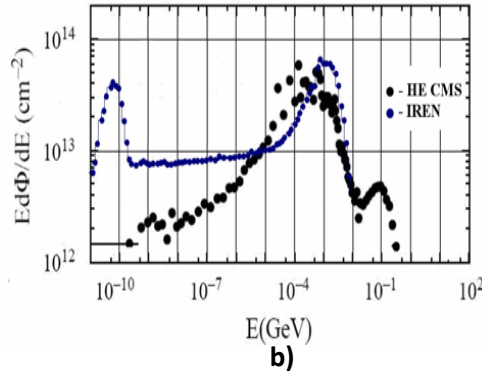


Figure 20. Results of the simulation of the dose rate ($\mu\text{ Sv/h}$) caused by the induced radioactivity of the HE absorber while LS1, LS2, LS3.

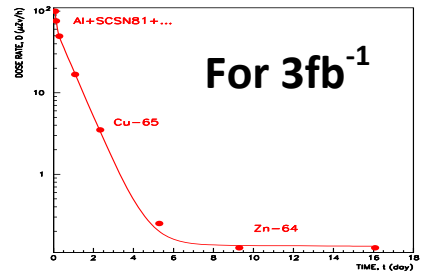
One more experimental result is related with the measurement of the megatitle dose rate due to the induced radioactivity by neutrons with fluence of $3 \cdot 10^{12} \text{ n/cm}^2$. The measurement was performed on IREN facility at JINR (Dubna). Figure 21a gives an external view of this setup. Figure 21b demonstrates a comparison of neutron spectra for IREN and the calculated one - in the area of the HE CMS. Figure 21c shows the dependence of the megatitle dose rate vs. time. Figure 21d shows the design of a megatitle fragment to test the induced activity.



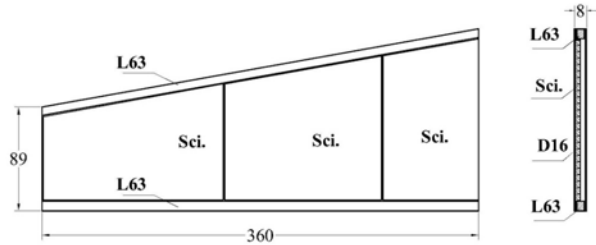
a)



b)



c)



d)

Figure 21. Measurement performed on IREN facility at JINR (Dubna).

The results of measurements of the induced activity allow one to evaluate the dependence of the dose rate (on the surface of the megatile of L0) vs. time for the following integral luminosities delivered by LHC: 200 fb^{-1} and 700 fb^{-1} (see Figure 22). The solid straight line indicates the level of safe conditions to work with megatile elements. It should be less than $3 \text{ } \mu\text{Sv/h}$ according to the CERN safety regulations.

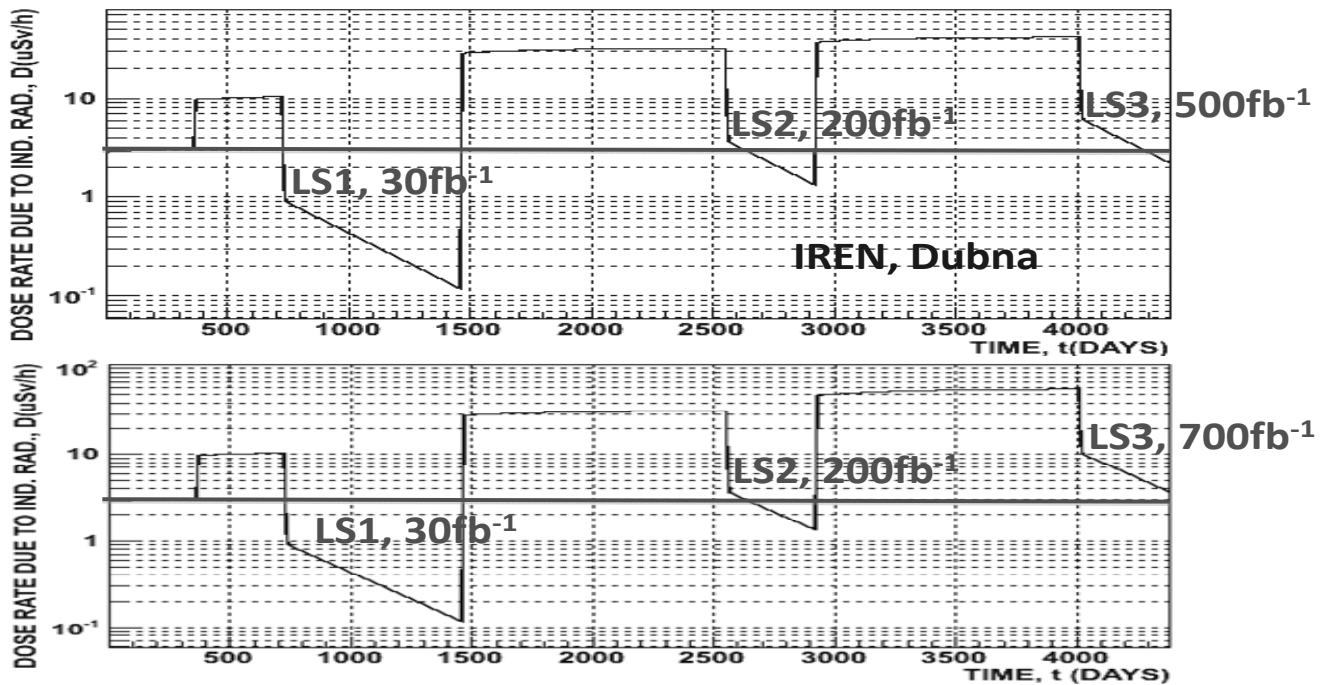


Figure 22. Dependence of the dose rate vs. time for the following integral luminosities delivered by LHC: 200 fb^{-1} and 700 fb^{-1} .

5. Summary.

The CMS scintillator-tile calorimeters (HB, HE, HO) have been in operation for many years and contributed a lot to the success of the CMS Physics Program. The technology of calorimeters is well understood. The main HE problem at HL LHC is radiation damage of scintillator tiles. A finger-strip plastic scintillator option has many advantages and is the cheapest way to keep excellent HE performance at high luminosity.

The HE dose simulations with FLUKA and MARS are of extreme importance for the upgrade strategy and should be continued to provide more details. For the finger-scintillator option the study of radiation damage of scintillators is also a key issue.

There are three issues to be considered:

- radiation damage of “fingers” up to $2500 - 3000 \text{ fb}^{-1}$ (end of LHC);
- radiation damage of existing sigma tiles at $500 - 700 \text{ fb}^{-1}$ (survivability by LS3);
- understanding of SCSN81/Y11 radiation damage at 30 fb^{-1} .

None of these issues has been considered yet but many important results have already been obtained. This study will also include gamma irradiation in the nitrogen atmosphere that, possibly, may reduce the damage depending on the dose rate. This program has to be completed in 2014 in order to be ready for TDR in spring 2015, if the upgrade is to be implemented during LS2. In parallel with RadDam study the preparation for tile production and megatile modification is in progress as well as the search for a new Rad hard scintillator.

References:

1. CMS Collaboration. “The CMS Experiment at the CERN LHC“, 2008 J. Inst. 3 S08004, DOI: 10.1088/1748-0221/3/08/S08004
2. CMS Collaboration. “Performance of the CMS hadron calorimeter with cosmic ray muons and LHC beam data”, 2010 J. Inst. 5 T03012, DOI: 10.1088/1748-0221/5/03/T03012, arXiv:0911.4991
3. CMS HCAL Collaboration. “Design, Performance, and Calibration of CMS Hadron Endcap Calorimeters”, CMS-NOTE-2008-010, 32 p.
4. E.Biagtan, E.Goldberg, J.Harmon and R.Stephens. “Effect of gamma radiation dose rate on the light output of commercial polymer scintillators”, Nuclear Instruments & Methods. 1994, v. B93, p. 296–301.
5. Technical proposal for the upgrade of the CMS detector through 2020, CMS U1TDR, 2011/06/01.
6. M. Guthoff and A. Dabrowski. “FLUKA simulations for HCAL”, DESY upgrade week, 3-7 June 2013 DESY Hamburg
<https://indico.cern.ch/getFile.py/access?contribId=0&resId=0&materialId=slides&confId=252240>
7. CMS collaboration. “CMS, The Hadron Calorimeter Technical Design Report,” CERN/LHCC 97-31 CMS TDR 2 (June 1997).
8. P. de Barbaro, H. Budd, A. Dyshkant, J. Gielata et al., Study of Light Yield and Radiation Hardness of Scintillators for CMS HCAL, CMS IN-2001/022 17 p.
9. S.V. Afanasiev, P. de Barbaro, I.A. Golutvin et al. "Improvement of radiation hardness of the sampling calorimeters based on plastic scintillators", Nuclear Instruments and Methods in Physics Research A 717 (2013) 11–13.
10. S.V. Afanasiev, I.F. Emeliantchik, I.A. Golutvin, L.G. Levchuk, A.V. Litomin et al., An improvement of a radiation hardness of the CMS Hadron Endcap Calorimeters under increased LHC luminosity, CERN CMS Note-2012/002 (2012) 8 p.
11. Victor Kryshkin, Victor Skvortsov. “Radiation hardness study of calorimeter active elements”, 2011, [arXiv:1108.5280v1](https://arxiv.org/abs/1108.5280v1) [physics.ins-det].
12. IBR-2 Pulsed Reactor. <http://flnp.jinr.ru/34/>

13. IREN Facility. <http://flnp.jinr.ru/35/>
14. LINAC <http://www.kipt.kharkov.ua/en/ihepnp.html>
15. S.W. Han et al. "Radiation hardness tests of scintillating tile/WLS fiber calorimeter modules", NIM A365 (1995) pp. 337 – 351.